Available online at www.sciencedirect.com
ScienceDirect
Biochimica et Biophysica Acta 1758 (2006) 1475–1482
BIOCHIMICA ET BIOPHYSICA ACTA
BBA
www.elsevier.com/locate/bbamem

The effect of binding of spider-derived antimicrobial peptides, oxyopinins, on lipid membranes

Kaoru Nomura [a,*], Gerardo Corzo [b]

[a] *Suntory Institute for Bioorganic Research, 1-1-1 Wakayamadai, Shimamoto-Cho, Mishima-Gun, Osaka 618-8503, Japan*
[b] *Institute of Biotechnology-UNAM, Av. Universidad 2001, Cuernavaca, Morelos, 62210, Mexico*

Received 7 December 2005; received in revised form 19 April 2006; accepted 19 April 2006
Available online 19 May 2006

Abstract

Oxyopinins (Oxki1 and Oxki2) are antimicrobial peptides isolated from the crude venom of the wolf spider *Oxyopes kitabensis*. The effect of oxyopinins on lipid bilayers was investigated using high-sensitivity titration calorimetry and ^{31}P solid-state NMR spectroscopy. High-sensitivity titration calorimetry experiments showed that the binding of oxyopinins was exothermic, and the binding enthalpies (ΔH) to 1-palmitoyl-2-oleoyl-*sn*-glycero-3-phosphatidylcholine (POPC) small unilamellar vesicles (SUVs) were −18.1 kcal/mol and −15.0 kcal/mol for Oxki1 and Oxki2, respectively, and peptide partition coefficient (K_p) was found to be 3.9×10^3 M^{-1}. ^{31}P NMR spectra of 1,2-dielaidoyl-*sn*-glycero-3-phosphoethanolamine (DEPE) membranes in the presence of oxyopinins indicated that they induced a positive curvature in lipid bilayers. The induced positive curvature was stronger in the presence of Oxki2 than in the presence of Oxki1. ^{31}P NMR spectra of phosphaditylcholine (PC) membranes in the presence of Oxki2 showed that Oxki2 produced micellization of membranes at low peptide concentrations, but unsaturated PC membranes or acidic phospholipids prevented micellization from occurring. Furthermore, ^{31}P NMR spectra using membrane lipids from *E. coli* suggested that Oxki1 was more disruptive to bacterial membranes than Oxki2. These results strongly correlate to the known biological activity of the oxyopinins.

Keywords: Spider-derived antimicrobial peptide; Membrane binding; Lipid bilayer; ^{31}P solid-state NMR; ITC; Curvature strain

1. Introduction

Polycationic antimicrobial peptides represent the chemical counterpart to the cell-mediated immune response in the innate host defense against pathogenic microorganisms [1,2]. They act as self-defense against other animals or pathogens or as weapons for capturing prey by forming channels or pores in the cell membrane, including cell permeation and a breakdown of cellular physiology. They have been found in various organisms, for example, PGLA [1] and magainin 2 [2] in the skin of frog, buforins [3] in the stomach tissue of toad, cecropin A [4], melittin [5], mastoparan X [6], ponericin [7], and pandinins [8] in venomous secretions of insects and scorpion, polyphemusins and tachyplesins [9] in the hemocyte of horse shoe crab, LL-37 [10] in the epithelial cell of human, and paradaxin [11] in mucosal secretion of fish. There are also newly designed antimicrobial peptides, for example, MSI-78 and $(KIGAKI)_3$ [12], that have stronger activity than naturally occurring ones for pharmaceutical development. These types of antimicrobial peptides are relatively small (2–6 kDa), amphipathic and basic peptides of variable length, sequence and structure. These peptides have been separated into two main categories according to whether or not they contain cysteines linked in disulfide bridges: (1) linear α-helical peptides, which adopt a random structure in dilute aqueous solution and form α-helices or an helix–bend–helix motif in organic solvents and upon contact with cell membrane

Abbreviations: CD, circular dichroism; DMPC, 1,2-dimyristoyl-*sn*-glycero-3-phosphatidylcholine; DMPG, 1,2-dimyristoyl-*sn*-glycero-3-phosphatidylglycerol; DEPE, 1,2-dielaidoyl-*sn*-glycero-3-phosphoethanolamine; H_{II}, inverted hexagonal phase; HPLC, high-performance liquid chromatography; ITC, isothermal titration calorimetry; L_α, lamellar phase; MALDI-TOF, matrix-assisted laser-desorption ionization-time-of-flight; MLV, multi-lamellar vesicles; NMR, nuclear magnetic resonance; ODS, octa decyl silica; PC, phosphaditylcholine; PE, phosphaditylethanolamine; PG, phosphatidylglycerol; POPC, 1-palmitoyl-2-oleoyl-*sn*-glycero-3-phosphatidylcholine; POPG, 1-palmitoyl-2-oleoyl-*sn*-glycero-3-phosphatidylglycerol; SUVs, small unilamellar vesicles

* Corresponding author. Tel.: +81 75 962 6152; fax: +81 75 962 2115.
E-mail address: nomura@sunbor.or.jp (K. Nomura).

0005-2736/$ - see front matter © 2006 Elsevier B.V. All rights reserved.
doi:10.1016/j.bbamem.2006.04.022

phospholipids [1–8,10–12], and (2) the β-sheet peptides, which comprise the α- and β-defensins, and the protegrin/tachyplesin group, which contain several disulfide bridges and adopt either a β-sheet or a β-hairpin fold [9]. The number of antimicrobial peptides described so far has increased considerably to more than 800, of which roughly more than half are linear α-helical peptides (http://www.bbcm.univ.trieste.it/~tossi/pag5.htm). Several mechanisms of membrane disruption have been proposed for antimicrobial peptides [13–26]. For example, melittin and pandinin2 insert into the membrane hydrophobic core with their average helical axis perpendicular to the membrane surface and rotate around the membrane normal [13–15]. Cecropin A and pandinin 1 lie at the surface of the bilayer and self-associates in a "carpet-like" manner [16,17]. Magainin2 and mastoparan X forms "toroidal pores" in lipid bilayers, where the inner and outer monolayers are associated via phospholipid lining, and the pores are formed by the lipid polar head groups and helix polar face [18,19].

Oxyopinins are large cationic peptides isolated from the crude venom of the wolf spider *Oxyopes kitabensis* [27]. Oxyopinin 1 (Oxki1) and Oxyopinin 2 (Oxki2) are composed of 48 and 37 residues, respectively. As shown by their helical wheel representations (Fig. 1), both oxyopinins are amphipathic and cationic peptides that have demonstrated high antimicrobial activity against a range of Gram-positive and Gram-negative bacteria. Although they have been chemically and biologically characterized, the binding and membrane disrupting mechanisms of the oxyopinins in lipid membranes have not yet been clarified.

In this study, we investigated the binding of oxyopinins to lipid membranes using ^{31}P solid-state NMR spectroscopy. Furthermore, we used CD spectroscopy and high-sensitivity titration calorimetry to investigate the binding of Oxki1 and Oxki2 to unilamellar phospholipid vesicles.

2. Materials and methods

2.1. Materials

Phospholipids, including the lipids from *E. coli* membranes, were purchased from Funakoshi (Tokyo, Japan) and used without further purification. The peptides Oxki1 and Oxki2 were chemically synthesized by solid-phase peptide synthesis using fluoren-9-ylmethoxycarbonyl (Fmoc) methodology on an Applied Biosystems 433A peptide synthesizer. Fmoc-Gln(tBu)-PEG resin (Watanabe Ltd., Hiroshima, Japan) was used for Oxki1 and Oxki2 to provide a free carboxyl group at the C-terminus. After synthesis, peptide deprotection, and cleavage from the resin, the crude peptides were dissolved in 30% acetonitrile solution and purified by reversed-phase HPLC on a semi-preparative C18 ODS column (10×250 mm, Nacalai Tesque, Kyoto, Japan). Cation exchange chromatography and C4 reversed-phase HPLC were further used to purify the peptides. The mass and purity of the peptides were confirmed by MALDI-TOF-MS.

2.2. Preparation of phospholipids vesicles

Small unilamellar vesicles (SUVs) for CD and ITC measurements were prepared as follows. A defined amount of lipid was dissolved in chloroform and dried first under nitrogen and then overnight under high vacuum. The lipid film was hydrated with 20 mM Tris buffer (100 mM NaCl, pH 7.6), and the lipid suspension was extensively vortex-mixed. Finally, the lipid dispersions were sonicated in ice water for 10 min using the titanium tip ultrasonicator until the solution became opalescent.

Multi-lamellar vesicles (MLVs) for NMR measurements were prepared as follows. The membrane system was made up of lipids and co-solubilized with the appropriate amounts of peptide to give the desired peptide-to-lipid (*P*/*L*) molar ratio in chloroform/methanol (2:1). After solvent evaporation under high vacuum overnight, the lipid film was hydrated with 20 mM Tris buffer (100 mM NaCl, pH 7.6), and the suspension was vortex-mixed extensively. The suspension was freeze-thawed for ten cycles and centrifuged. The supernatant was removed, and the water content was adjusted to ~80% (w/w), and the suspension was transferred to NMR tubes.

2.3. CD measurements

CD spectra of the peptides were recorded at room temperature on a Jasco J-725 spectropolarimeter (Jasco, Japan) using a 1-mm-path-length cell. The spectra were measured between 200 and 250 nm in 20 mM Tris buffer (100 mM NaCl, pH 7.6) or in the presence of 10 mM POPC SUVs (same buffer) and average blank spectra were subtracted. Data were collected at 0.1 nm with a scan rate of 100 nm/min and a time constant of 0.5 s. The concentration of the peptides was 50 μM. The helicity of the peptides, f_H, was determined from the mean residue ellipticity [Θ] at a wavelength of 222 nm according to the empirical method of Rohl and Baldwin [28].

2.4. High-sensitivity titration calorimetry

Isothermal titration calorimetry was performed using a MicroCal VP high-sensitivity titration calorimeter (MicroCal, Northampton, MA) according to Wiseman et al. [29]. To eliminate air bubbles, solutions were degassed under vacuum prior to use. The calorimeter was calibrated electrically. The data were acquired by computer software developed by MicroCal. In control experiments, the corresponding peptide solution (or vesicle suspension) was injected into buffer (20 mM Tris–HCl, 100 mM NaCl, pH 7.6). Heats of dilution were subtracted from the actual measurement.

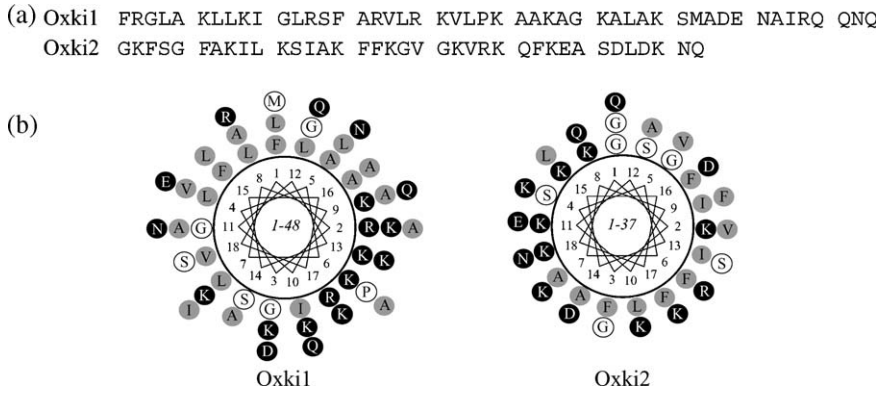

Fig. 1. (a) Amino acid sequences of Oxki1 and Oxki2. (b)Helical wheel projections of Oxki1 and Oxki2. Charged, neutral, and hydrophobic residues are shown in black, white, and gray, respectively.

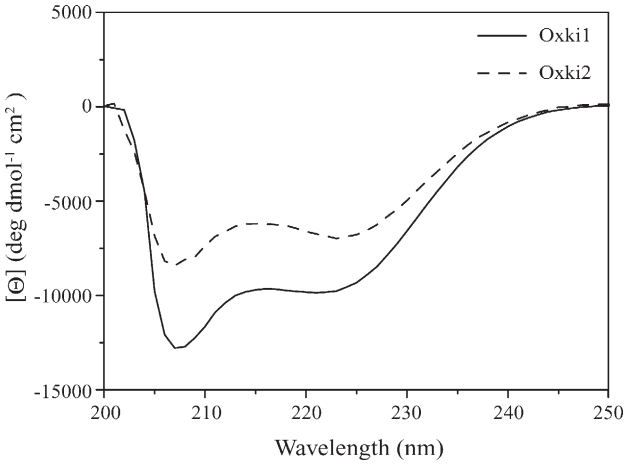

Fig. 2. CD spectra of synthetic Oxki1 and Oxki2 in 20 mM Tris–HCl buffer plus 10 mM POPC SUVs, pH 7.6.

2.5. Solid-state NMR spectroscopy

All solid-state NMR spectra were acquired on a CMX Infinity 300 spectrometer (Chemagnetics, Varian, Palo Alto, CA) operating at a proton resonance frequency of 300 MHz. ^{31}P spectra were acquired using a 5-μs single excitation pulse with 30-kHz continuous wave (CW) ^{1}H decoupling during acquisition. The dwell time was 50 μs, and 100–2000 transients were accumulated for each free induction decay (FID) with a 3-s relaxation delay. The ^{31}P chemical shifts were referenced externally to 85% H_3PO_4 (0 ppm).

3. Results

3.1. Circular dichroism

CD spectroscopy was used to study the secondary structures of Oxki1 and Oxki2. Fig. 2 shows the CD spectra of both peptides in the presence of 20 mM Tris–HCl buffer plus 10 mM POPC SUVs. The CD spectra indicated the formation of α-helical structures with double minima around 208 and 222 nm. The helicity of the peptides, f_H, determined from the mean residue ellipticity at 222 nm, $[\Theta]_{222}$, was found to be 29.3% for Oxki1 and 21.3% for Oxki2. Similar CD spectra of the oxyopinins have been previously observed in 60% solutions of TFE, a solvent that mimics hydrophobic environments [27]. In the presence of 20 mM Tris–HCl buffer, the oxyopinins adopted unordered structures (spectra not shown).

3.2. Binding enthalpy measured with isothermal titration calorimetry

We have used high-sensitivity calorimetry to investigate the binding of oxyopinins to phospholipid vesicles. Fig. 3a shows a 4-μl step titration of 200 μM Oxki2 peptide solution into a suspension of 15 mM POPC SUVs at 30 °C. Since the heat of reaction (h_i) was virtually identical in each 4-μl injection, it was concluded that the injected peptide was completely bound to the POPC vesicles (Fig. 3b). The average heat of injection was −12.4 μcal. As a control, the same peptide solution was injected into a buffer solution (data not shown), yielding a heat of dilution of −0.4 μcal. This was subtracted from the actual measurement, yielding an average heat of reaction of $\delta h = -12.0$ μcal. The enthalpy of binding into the POPC membranes was calculated under the assumption that all injected peptide was completely bound to the phospholipid vesicles. The enthalpies were −18.1 and −15.0 kcal/mol for Oxki1 and Oxki2, respectively.

Fig. 3c displays a 10-μl step titration of 30 mM POPC SUV suspension into an Oxki2 peptide solution ($c_p^0 = 6$ μM) at 30 °C. Here, each 10-μl injection gave rise to an exothermic heat of reaction (h_i), which decreased in magnitude with consecutive injections. As a control, a suspension of 30 mM POPC SUVs was injected into the buffer solution (data not shown), yielding a

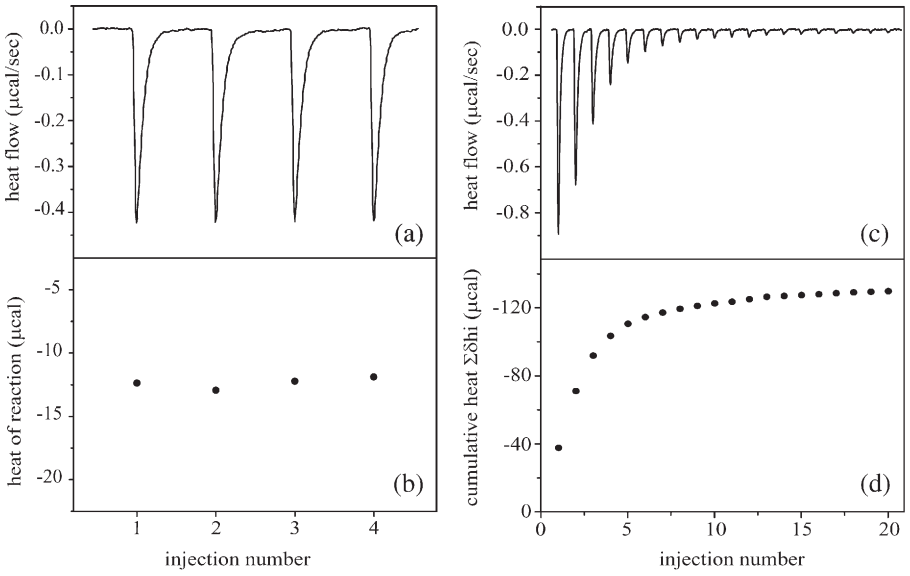

Fig. 3. Titration calorimetry of the binding of Oxki2 to POPC SUVs. (a) Calorimeter tracings. A series of 4-μl injections of 200 μM peptide solution in the reaction cell (1.4266 ml) containing 15 mM POPC SUVs. (b) The heat of reaction of the experiment shown in (a). (c) Calorimeter tracings. A series of 10-μl injections of 30 mM POPC SUVs suspension in the reaction cell containing a 6 μM peptide solution. (d) Cumulative heat of reaction of the experiment shown in panel (c).

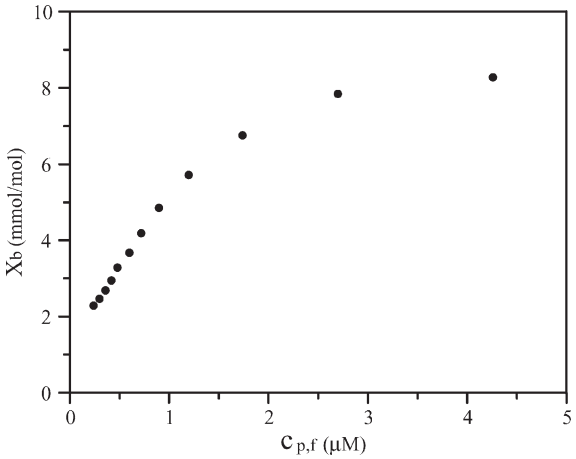

Fig. 4. Binding of Oxki2 to POPC SUVs. The bound peptide to lipid (X_b=mmolOxki2/mol POPC SUVs) is plotted as a function of the free peptide concentration ($c_{p,f}$). A 6 μM peptide solution, at 30 °C, was titrated with SUVs.

heat of dilution of −0.3 μcal, which was subtracted from the actual measurement (Fig. 3d). The cumulative heat of reaction after i injections according to Eq. (1) is shown in Fig. 3d.

$$\delta H_i = \sum_{k=1}^{i} \delta h_k \quad (1)$$

The reaction had largely ceased after 20 injections, and all peptide was bound to the lipid vesicles. The accumulative heat was δH_{20}=130.0 μcal, and the molar heat of binding, which was exothermic, was $\Delta H = \delta H_{10}/n_p^0 = -15.2$ kcal/mol. This value was in good agreement with those determined in Fig. 3a and b. Wenk et al. [30] have shown similar results using ITC experiments to investigate the binding of magainin 2 amide to phospholipid vesicles [30]. Moreover, the isothermal titration calorimetry experiments showed that at low P/L ratio [$(P/L)^0$=1/27000] Oxki2 was bound immediately to the POPC vesicles, and that at high P/L ratio [$(P/L)^0$=1/35] the binding to POPC vesicles was completely saturated.

Fig. 4 shows the binding of Oxki2 to POPC SUVs (X_b) as a function of the free Oxki2 concentration. Although the lipid bilayer was composed of neutral POPC phospholipids, the binding isotherm was linear up to 6 mmol peptide/mol POPC and membranes were saturated at 8 mmol peptide/mol POPC. This can be explained as follows: Since the binding of the first Oxki2 molecules (which possesses a positive charge) to the neutral membrane creates a positively charged outer surface, the binding of further molecules becomes more difficult due to the electrostatic repulsion [31]. The peptide partition coefficient (K_p) was determined from the slope of the initial, linear portion of the binding isotherms (X_b), and it was found to be $K_p = 3.9 \times 10^3$ M^{-1}.

3.3. Peptide — DEPE lipid membrane interactions and peptide induced curvature strain

To examine the effect of Oxki1 and Oxki2 on DEPE lipid bilayers, and their abilities to induce curvature strain on lipid bilayers, ^{31}P NMR spectra of DEPE lipid bilayers in the absence and presence of the oxyopinins were observed at various temperatures under static conditions. Fig. 5a shows the ^{31}P NMR spectra of DEPE lipid bilayers at various temperatures in the absence of peptides. At 50 °C, an axially symmetric and motionally averaged powder pattern was observed. This pattern indicated that the lipids formed MLVs. When the temperature was raised to 55 °C, a peak around 6 ppm was observed superimposed on the MLV component, indicating the coexistence of an inverted hexagonal phase [32] and a Lα phase. At 60 and 70 °C, only the inverted hexagonal phase was observed. Since the Lα-H_{II} phase transition temperature (T_H) of DEPE is around 60 °C [33], this temperature dependence was reasonable. In the presence of Oxki1 (Fig. 5b and c), the spectrum exhibited a similar MLV phase as in the absence of peptide at 50 °C; however, the higher the concentration of Oxki1 the higher the T_H

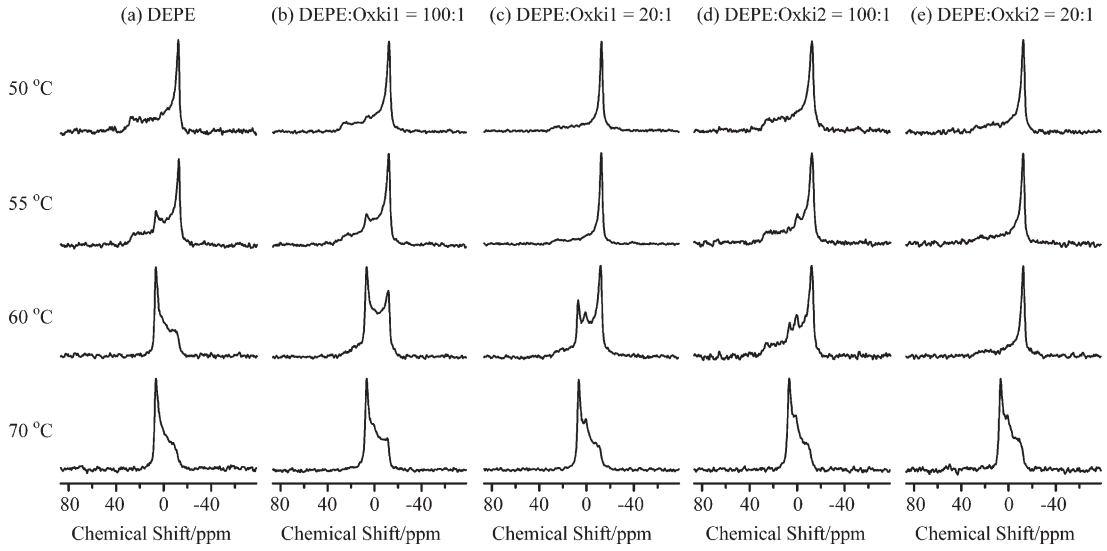

Fig. 5. ^{31}P NMR spectra of dispersions of DEPE in the absence (a) and presence of Oxki1 (b, c) and Oxki2 (d, e) at various temperatures. The peptide/DEPE ratio was 1/100 for panels (b, d) and 1/20 for panels (c, e).

value of DEPE was, implying that Oxki1 imposed a positive curvature strain on the membrane according to Wieprecht et al. and Wildman et al. [34,35]. Furthermore, in the presence of Oxki2 (Fig. 5d and e), the temperature dependence of DEPE showed a higher T_H value than that in the presence of Oxki1 under the same peptide/lipid molar ratio, implying that Oxki2 imposed a stronger positive curvature strain on the membrane than did Oxki1.

3.4. Oxki2-PC lipid membrane interactions

In order to examine the effects of Oxki2 on PC lipid membranes, ^{31}P NMR spectra of PC lipid membranes in the presence of Oxki2 were measured under static conditions. Fig. 6a shows ^{31}P NMR spectra of dispersions of DMPC membranes (T_m ~23 °C) [36] at 30 °C containing various amounts of Oxki2. At P/L=1/100, sharp isotropic components were observed indicating the coexistence of an isotropic phase and a Lα phase. At P/L=1/40 and 1/20, only an isotropic narrow signal was observed. This isotropic component may be attributed to fast isotopic tumbling of the phospholipids, which may be caused by the formation of micelles, small unilamellar vesicles or small discoidal bilayers. A similar sharp isotropic peak was observed on the DPPC membrane in the presence of Oxki2 at 50 °C (T_m ~42 °C) [36] at a molar ratio of Oxki2/DPPC=1/20 (spectrum not shown). Fig. 6b shows the ^{31}P NMR spectrum of dispersions of DMPC/DMPG (4:1) membranes at 30 °C containing Oxki2 at P/L=1/20. No isotropic components were observed, indicating that micellization was prevented due to the negatively charged DMPG. The head groups of DMPG most likely interacted with the positively charged lysine or arginine residues in Oxki2. Fig. 6c shows the ^{31}P NMR spectrum of dispersions of POPC lipid bilayers at 20 °C (T_m ~−5 °C) [37] containing Oxki2 at P/L=1/20. Although a small isotropic signal was observed superimposed on a bilayer component, it was much smaller than that of Fig. 6a. Also, almost all part of the spectrum showed an MLV component, suggesting that micellization was prevented due to the *cis*-double bond present in the hydrocarbon chain of POPC.

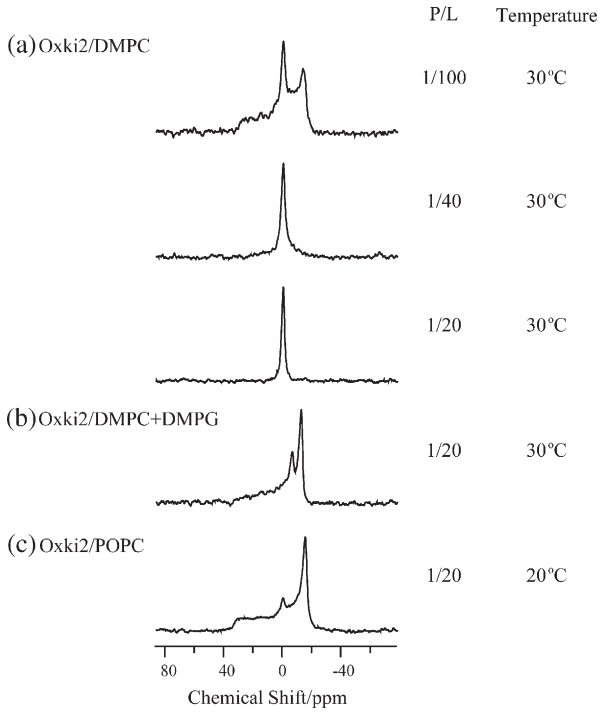

Fig. 6. Effect of Oxki2 at various concentrations and temperatures on the ^{31}P NMR spectra of phospholipid dispersions composed of (a) DMPC, (b) DMPC/DMPG (4:1), and (c) POPC.

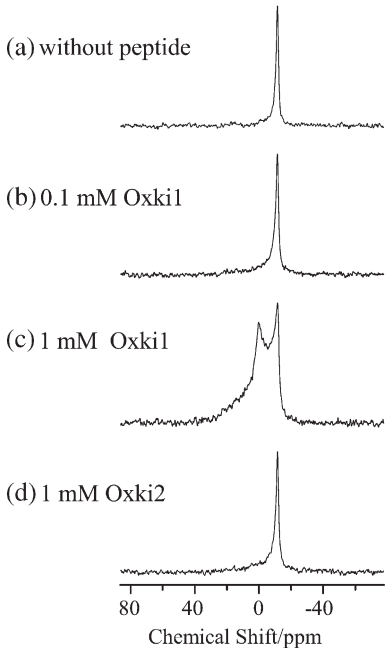

Fig. 7. ^{31}P NMR spectra of *E. coli* total lipid bilayers in the absence (a) and presence of Oxki1 (b, c) and Oxki2 (d) at 30 °C. The peptide concentrations were 0.1 mM for (b) and 1 mM for (c) and (d). Lipid concentrations were 5% w/w.

3.5. Oxyopinins and bacterial membrane interactions

To investigate the effects of the oxyopinins on bacterial membranes, ^{31}P NMR spectra of *E. coli* total lipid bilayers were observed in the absence and presence of Oxki1 and Oxki2. In the absence of peptides, an axially symmetric motionally averaged powder pattern was observed (Fig. 7a). When Oxki1 was added to the bilayers, an isotropic peak was observed at a peptide concentration of 1 mM (Fig. 7b and c). However, when Oxki2 was added to the bilayers at 1 mM concentration, no isotropic peaks were observed, and only the axially symmetric and magnetically aligned powder pattern was present (Fig. 7d). These results suggest that Oxki1 is more disruptive to bacterial membranes than Oxki2.

4. Discussion

The CD spectra of Oxki1 and Oxki2 (Fig. 2) showed that both peptides adopt an α-helical structure in lipid membranes. The enthalpic contribution of helix formation at the membrane surface of POPC/POPG (3:1) SUVs had been estimated previously by Wieprecht et al. as ΔH_{helix}=−0.72 kcal/mol [38]. According

to it, the contribution of helix formation to the POPC SUVs binding process is defined by the equation (ΔH_{helix}) (number of residue) (helicity); therefore, for oxyopinins were $(-0.72)\times 48\times 0.293=-10.1$, and $(-0.72)\times 37\times 0.213=-5.7$ kcal/mol for Oxki1 and Oxki2, respectively. The helix formation accounts for 56% and 38% of the total binding enthalpy of these peptides ($\Delta H_{Oxki1}=-18.1$ kcal/mol and $\Delta H_{Oxki2}=-15.0$ kcal/mol). The enthalpic contribution of helix formation and its percent of contribution to total binding for magainin 2 amide is −12.2 kcal/mol and 77% [38], for mellitin −13.7 kcal/mol and 77% [38], and for MSI-843 −2.6 kcal/mol and 60% [39], respectively. Comparing these values with those found for oxyopinins, the enthalpic contribution of helix formation was smaller for the oxyopinins, and this may be attributed to the low helicity of Oxki1 and Oxki2 as shown by the CD spectra. The non-helix contribution to ΔH (ΔH_0) was then −8.0 kcal/mol and −9.3 kcal/mol for Oxki1 and Oxki2, respectively. These values might be due to pore formation and disintegration of the peptides [30].

In neutral POPC membranes, the partition coefficient for Oxki2 was 3.9×10^3 M^{-1}, which suggest that Oxki2 interacts weakly. In neutral POPC membranes, the partition coefficient for polyphemusin, an antimicrobial peptide, was 2.7×10^3 M^{-1} [26], and that for Cyclosporin A, an immunosuppressive agent, was 4.3×10^3 M^{-1} [31]. On the other hand, in negatively charged POPC/POPG (3:1) membranes, the partition coefficient for polyphemusin was 31×10^3 M^{-1} [26]. Comparing these values, the low affinity of Oxki2 for neutral POPC membranes is similar to other antimicrobial agents, and Oxki2 might show greater affinity to negatively charged membranes.

The ^{31}P NMR spectra of DEPE membranes (Fig. 5) suggested that both Oxki1 and Oxki2 induced positive curvature strain in lipid bilayers. Belokoneva et al. [40] reported that the Oxki1-induced calcein release from PC SUVs was significantly inhibited by the incorporation of PE, a negative curvature inducer, into the PC calcein-loaded SUVs. These results indicated that the positive curvature favored pore formation by Oxki1. Similarly, magainin2 is known to form toroidal pores, which are caused by positive curvature stress induced by the peptide on lipid membranes [41,42]. Therefore, it seems that Oxki1 and Oxki2 are likely to form toroidal pores by inducing positive curvature strain in lipid membranes, as does magainin 2.

Brown [43] mentioned that the change in the curvature in lipid bilayers could be caused for a conformational change of proteins, as in the case of the conformational change of rhodopsin from MI to MII state. In rhodopsin, the MI state favored the lamellar phase with zero spontaneous curvature; on the other hand, elongation or protrusion of rhodopsin at the MII state induce the reverse hexagonal (H_{II}) phase with a negative interfacial curvature in lipid bilayers. Similarly, the presence of oxyopinins may induce the imbalance of attractive and repulsive force at the level of the lipids head group and acyl chains in lipid bilayers; and then, they form the non-lamellar phase with a positive interfacial curvature of lipid bilayer, which might be at a free energy minimum in lipid–membrane peptide interaction.

The ^{31}P NMR spectra of DMPC membranes (Fig. 6) in the presence of Oxki2 showed that Oxki2 promotes micellization of membranes. On the other hand, the micellization by Oxki1 and Oxki2 did not occur on DEPE membranes (Fig. 5) suggesting that the negative curvature of DEPE membranes prevented micellization by the oxyopinins. These results are strongly correlated to the biological activity of both peptides [27]. It was observed that the hemolytic and pore-forming activities of Oxki1 and Oxki2 depend on the source of red blood cells, which were strongly associated with the percentages of PC in the total membrane phospholipids of 41, 23, and 1% for Guinea pig, pig, and sheep red blood cells, respectively [44,45]. The hemolytic and pore-forming activities of Oxki1 and Oxki2 were higher in Guinea pig > pig > sheep [11]. Thus, erythrocytes having PC-rich cell membranes are more susceptible to the hemolysis induced by the oxyopinins. Furthermore, Oxki1 and Oxki2 were more lytic toward PC vesicles than towards PE and PA [11]. The pore-forming activities of oxyopinins may be explained by their abilities to induce positive curvature strains in lipid bilayers.

Cholate molecules are also known to disrupt lipid membranes by a strong ability to induce a positive curvature strain in lipid bilayers [46]. Thurmond et al. [46] reported that cholate changes the curvature of DOPE from negative (H_{II} phase), through zero (Lα phase) and finally to a phase of positive curvature (micellar solution) at high water content. The cholate molecule consists of a rigid steroid fused ring system, which is roughly planar, in which one side is hydrophobic and the other one is hydrophilic. The strong ability to induce the positive curvature strain was explained in terms of its unique structure, which have tendency to lie flat on the lipid aggregate surface and increase the effective interfacial area of the polar head groups. Although oxyopinins do not have such rigid ring system, they might lie on the lipid membrane due to basic and acidic amino acid-rich character, and it may be the reason for their strong ability to induce positive curvature.

E. coli total lipid contains (w/w) approximately 57.5% PE, 15.1% PG, 9.8% Cardiolipin, and 17.6% other lipids [47,48]. Moreover, it was reported that Oxki1 kills *E. coli* cells at lower concentrations than that of Oxki2 [27]. The fact that Oxki1 showed stronger antimicrobial activity toward *E. coli* than Oxki2 also correlates to our NMR results in Fig. 7. Therefore, the stronger antimicrobial activity of Oxki1 may also originate from the stronger ability of Oxki1 to disrupt bacterial membranes.

The typical “toroidal pore” forming antimicrobial peptides, PGLa (GMASK AGAIA GKIAK VALKA L-NH_2)[1] and magainin 2 (GIGKF LHSAK KFGKA FVGEI MNS)[2], do not have tryptophan and tyrosine residues. These residues are known to reside preferentially near the membrane surface [49]. Therefore, the ability to induce positive curvature strain of oxyopinins might be due to the absence of the amino acid residues tryptophan and tyrosine. Furthermore, the stronger ability of Oxki2 to induce a positive curvature strain might be due to the absence of a central proline residue. For example, the transmembrane type peptides, melittin and pandinin 2, have a proline residue in the middle of the alpha-chain. On the other hand, “toroidal pore” forming antimicrobial peptides, PGLa and magainin 2, have no proline residue. Kobayashi et al. had reported that a Pro → Ala substitution in buforin 2 (TRSSR AGLQW PVGRV HRLLR K)[3] caused buforin 2 to show magainin-like properties in terms of conformation, translocation efficiency, and leakage coupled lipid

flip-flop [50]. Therefore, a central proline residue could be a very important factor for curvature strains induced by these antimicrobial peptides.

References

[1] W. Hoffmann, K. Richter, G. Kreil, A novel peptide designated PYLa and its precursor as predicted from cloned mRNA of Xenopus laevis skin, EMBO J. 2 (1983) 711–714.

[2] M. Zasloff, Magainins, a class of antimicrobial peptides from *Xenopus* skin: isolation, characterization of two active forms, and partial cDNA sequence of a precursor, Proc. Natl. Acad. Sci. U. S. A. 84 (1987) 5449–5453.

[3] C.B. Park, M.S. Kim, S.C. Kim, A novel antimicrobial peptide from *Bufo bufo* gargarizans, Biochem. Biophys. Res. Commun. 218 (1996) 408–413.

[4] T.A. Holak, A. Engstroem, P.J. Kraulis, G. Lindeberg, H. Bennich, T.A. Jones, A.M. Gronenborn, G.M. Clore, The solution conformation of the antibacterial peptide cecropin A: a nuclear magnetic resonance and dynamical simulated annealing study, Biochemistry 27 (1988) 7620–7629.

[5] J.F. Fennell, W.H. Shipman, L.J. Cole, Antibacterial action of melittin, a polypeptide from bee venom, Proc. Soc. Exp. Biol. Med. 127 (1968) 707–710.

[6] Y. Hirai, T. Yasuhara, H. Yoshida, T. Nakajima, M. Fujino, C. Kitada, A new mast cell degranulating peptide "mastoparan" in the venom of *Vespula lewisii*, Chem. Pharm. Bull. 27 (1979) 1942–1944.

[7] J. Orivel, V. Redeker, J.P. Le Caer, F. Krier, A.M. Revol-Junelle, A. Longeon, A. Chaffotte, A. Dejean, J. Rossier, Ponericins, new antibacterial and insecticidal peptides from the venom of the ant *Pachycondyla goeldii*, J. Biol. Chem. 276 (2001) 17823–17829.

[8] G. Corzo, P. Escoubas, E. Villegas, K.J. Barnham, W. HE, R.S. Norton, T. Nakajima, Characterization of unique amphipathic antimicrobial peptides from venom of the scorpion *Pandinus imperator*, Biochem. J. 359 (2001) 35–45.

[9] T. Miyata, F. Tokunaga, T. Yonega, K. Yoshikawa, S. Iwanaga, M. Niwa, T. Takao, Y. Shimonishi, Antimicrobial peptides, isolated from horseshoe crab hemocytes, tachyplesin II, and polyphemusins I and II: chemical structures and biological activity, J. Biochem. 106 (1989) 663–668.

[10] G.H. Gudmundsson, B. Agerberth, J. Odeberg, T. Bergman, B. Olsson, R. Salcedo, The human gene FALL39 and processing of the cathelin precursor to the antibacterial peptide LL-37 in granulocytes, Eur. J. Biochem. 238 (1996) 325–332.

[11] P. Lazarovici, N. Primor, L.M. Loew, Purification and pore-forming activity of two hydrophobic polypeptides from the secretion of the Red Sea Moses sole, J. Biol. Chem. 261 (1986) 16704–16713.

[12] W.L. Maloy, U.P. Kari, Structure-activity studies on magainins and other host defense peptides, Biopolymers 37 (1995) 105–122.

[13] A. Naito, T. Nagao, K. Norisada, T. Mizuno, S. Tuzi, H. Saito, Conformation and dynamics of melittin bound to magnetically oriented lipid bilayers by solid-state ^{31}P and ^{13}C NMR spectroscopy, Biophys. J. 78 (2000) 2405–2417.

[14] S. Toraya, K. Nishimura, A. Naito, Dynamic structure of vesicle-bond melittin in a variety of lipid chain lengths by solid-state NMR, Biophys. J. 87 (2004) 3323–3335.

[15] K. Nomura, G. Corzo, T. Nakajima, T. Iwashita, Orientation and pore-forming mechanism of a scorpion pore-forming peptide bound to magnetically oriented lipid bilayers, Biophys. J. 87 (2004) 2497–2507.

[16] F.M. Marassi, S.J. Opella, P. Juvvadi, R.B. Merrifield, Orientation of cecropin A helices in phospholipid bilayers determined by solid-state NMR spectroscopy, Biophys. J. 77 (1999) 3152–3155.

[17] K. Nomura, G. Ferrat, T. Nakajima, H. Darbon, T. Iwashita, G. Corzo, Induction of morphological changes in model lipid membranes and the mechanism of membrane disruption by a large scorpion-derived pore-forming peptide, Biophys. J. 89 (2005).

[18] K. Matsuzaki, K. Sugishita, N. Ishibe, M. Ueha, S. Nakata, K. Miyajima, R.M. Epand, Relationship of membrane curvature to the formation of pores by magainin 2, Biochemistry 37 (1998) 11856–11863.

[19] K. Matsuzaki, S. Yoneyma, O. Murase, K. Miyajima, Transbilayer transport of ions and lipids coupled with mastoparan X translocation, Biochemistry 35 (1996) 8450–8456.

[20] O. Toke, R.D. O'Connor, T.K. Weldeghiorghis, W.L. Maloy, R.W. Glaser, A.S. Ulrich, J. Schaefer, Structure of $(KIAGKIA)_3$ aggregates in phospholipid bilayers by solid-state NMR, Biophys. J. 87 (2004) 675–687.

[21] F. Porcelli, B. Buck, D.-K. Lee, K.J. Hallock, A. Ramamoorthy, G. Veglia, Structure and orientation of pardaxin determined by NMR, experiments in model membranes,, J. Biol. Chem. 279 (2004) 45815–45823.

[22] K.J. Hallock, D.-K. Lee, A. Ramamoorthy, MSI-78, an analogue of the magainin antimicrobial peptides, disrupts lipid bilayer structure via positive curvature strain, Biophys. J. 84 (2003) 3052–3060.

[23] A. Mecke, D.-K. Lee, A. Ramamoorthy, B.G. Orr, M.M. Banaszak Holl, Membrane thinning due to antimicrobial peptide binding: an atomic force microscopy study of MSI-78 in lipid bilayers, Biophys. J. 89 (2005) 4043–4050.

[24] R.W. Glaser, C. Sachse, U.H.N. Dürr, P. Wadhwani, S. Afonin, E. Strandberg, A.S. Ulrich, Concentration-dependent realignment of the antimicrobial peptide PGLa in lipid membranes observed by solid-state ^{19}F-NMR, Biophys. J. 88 (2005) 3392–3397.

[25] P.C. Dave, E. Billington, Y.-L. Pan, S.K. Straus, Interaction of alamethicin with ether-linked phospholipid bilayers: oriented circular dichroism, ^{31}P solid-state NMR, and differential scanning calorimetry studies, Biophys. J. 89 (2005) 2434–2442.

[26] J.P.S. Powers, A. Tan, A. Ramamoorthy, R.E.W. Hancock, Solution structure and interaction of the antimicrobial polyphemusins with lipid membranes, Biochemistry 44 (2005) 15504–15513.

[27] G. Corzo, E. Villegas, F.G. Lagunas, L.D. Possani, O.S. Belokoneva, T. Nakajima, Oxyopinins, large amphipathic peptides isolated from the venom of the wolf spider *Oxyopes kitabensis* with cytolytic properties and positive insecticidal cooperativity with spider neurotoxins, J. Biol. Chem. 277 (2002) 23627–23637.

[28] C.A. Rohl, R.L. Baldwin, Comparison of NH exchange and circular dichroism as techniques for measuring the parameters of the helix-coil transition in peptides, Biochemistry 36 (1997) 8435–8442.

[29] T. Wiseman, S. Williston, J.F. Brandts, L.N. Lin, Rapid measurement of bonding constants and heats of binding using a new titration calorimeter, Anal. Biochem. 179 (1989) 131–137.

[30] M.R. Wenk, J. Seelig, Magainin 2 amide interaction with lipid membranes: calorimetric detection of peptide binding and pore formation, Biochemistry 37 (1998) 3909–3916.

[31] U. Schote, P. Ganz, A. Fahr, J. Seelig, Interaction of cyclosporines with lipid membranes as studied by solid-state nuclear magnetic resonance spectroscopy and high-sensitivity titration calorimetry, J. Pharm. Sci. 91 (2002) 856–867.

[32] P.R. Cullis, M.J. Hope, Effect of fusogenic agent on membrane structure of erythrocyte ghosts and the mechanism of membrane fusion, Nature 271 (1978) 672–674.

[33] R.M. Epand, Diacylglycerols, lysolecithin, or hydrocarbons markedly alter the bilayer to hexagonal phase transition temperature of phosphatidylethanolamines, Biochemistry 24 (1985) 7092–7095.

[34] T. Wieprecht, M. Dathe, R.M. Epand, M. Beyermann, E. Krause, W.L. Maloy, D.L. MacDonald, M. Bienert, Modulation of membrane activity of amphipathic, antibacterial peptides by slight modifications of the hydrophobic moment, Biochemistry 36 (1997) 12869–12880.

[35] K.A. Henzler Wildman, D.-K. Lee, A. Ramamoorthy, Mechanism of lipid bilayer disruption by the human antimicrobial peptide, LL-37, Biochemistry 42 (2003) 6545–6558.

[36] B.A. Lewis, D.M. Engelman, Lipid bilayer thickness varies linearly with acyl chain length in fluid phosphatidylcholine vesicles, J. Mol. Biol. 166 (1983) 211–217.

[37] J. Seelig, N. Waespe-Sarcevic, Molecular order in *cis* and *trans* unsaturated phospholipid bilayers, Biochemistry 17 (1978) 3310–3315.

[38] T. Wieprecht, O. Apostolov, M. Beyermann, J. Seelig, Thermodynamics of the alpha-helix-coil transition of amphipathic peptides in a membrane environment: implications for the peptide-membrane binding equilibrium, J. Mol. Biol. 294 (1999) 785–794.

[39] S. Thennarasu, D.-K. Lee, A. Tan, U.P. Kari, A. Ramamoorthy, Antimicrobial activity and membrane selective interactions of a synthetic lipopeptide MSI-843, Biochim. Biophys. Acta 1711 (2005) 49–58.

[40] O.S. Belokoneva, H. Satake, E.L. Mal'tseva, N.P. Pal'mina, E. Villegas, T. Nakajima, G. Corzo, Pore formation of phospholipid membranes by the

action of two hemolytic arachnid peptides of different size, Biochim. Biophys. Acta 1664 (2004) 182–188.
[41] K. Matsuzaki, O. Murase, N. Fujii, K. Miyajima, An antimicrobial peptide, magainin 2, induced rapid flip-flop of phospholipids coupled with pore formation and peptide translocation, Biochemistry 35 (1996) 11361–11368.
[42] S. Ludtke, K. He, W.T. Heller, T.A. Harroun, L. Yang, H.W. Huang, Membrane pores induced by magainin, Biochemistry 35 (1996) 13723–13728.
[43] M.F. Brown, Modulation of rhodopsin function by properties of the membrane bilayer, Chem. Phys. Lipids 73 (1994) 159–180.
[44] G.J. Nelson, Lipid composition of erythrocytes in various mammalian species, Biochim. Biophys. Acta 144 (1967) 221–232.
[45] D.A. White, Form and function of phospholipids, in: B. Ansell, R.M.C. Dawson, J.N. Hawthorne (Eds.), Phospholipids: Chemistry, Metabolism and Function, Elsevier, Amsterdam, 1973, pp. 441–482.
[46] R.L. Thurmond, G. Lindblom, M.F. Brown, Effect of bile salts on monolayer curvature of a phosphatidylethanolamine/water model membrane system, Biophys. J. 60 (1991) 728–732.
[47] M.J. Newman, T.H. Wilson, Solubilization and reconstitution of the lactose transport system from Escherichia coli, J. Biol. Chem. 255 (1980) 10583–10586.
[48] Y. Kagawa, E. Rackeer, Partial resolution of the enzymes catalyzing oxidative phosphorylation, J. Biol. Chem. 246 (1971) 5477–5487.
[49] W.M. Yau, W.C. Wimley, K. Gawrisch, S.H. White, The preference of tryptophan for membrane interfaces, Biochemistry 37 (1998) 14713–14718.
[50] S. Kobayashi, K. Takeshima, C.B. Park, S.C. Kim, K. Matsuzaki, Interaction of the nobel antimicrobial peptide buforin 2 with lipid bilayers: proline as a translocation promoting factor, Biochemistry 39 (2000) 8648–8654.